EVOLUTION OF PARAMETERS OF NONLINEAR POSITION CONTROL FOR DYNAMIC MODEL OF MOBILE ROBOT WITH FRICTION

Bakir Lacevic, Jasmin Velagic and Mujo Hebibovic

University of Sarajevo, Faculty of Electrical Engineering
Zmaja od Bosne bb, 71000 Sarajevo, Bosnia and Herzegovina
e-mails: bakir.lacevic@etf.unsa.ba, jasmin.velagic@etf.unsa.ba, mujohebi@hotmail.com

Abstract: In this paper, we propose two level control system for a mobile robot. The first level subsystem deals with the control of the linear and angular volocities using a multivariable PI controller described with a full matrix. The position control of the mobile robot represents the second level control, which is nonlinear. The nonlinear control design is implemented by a modified backstepping algorithm whose parameters are adjusted by a genetic algorithm, which is a robust nonlinear optimization method. The performance of the proposed system is investigated using a dynamic model of a nonholonomic mobile robot with friction. We present a new dynamic model in which the angular velocities of wheels are main variables. Simulation results show the good quality of position tracking capabilities a mobile robot with the various viscous friction torques.

Keywords: mobile robot dynamics, position control, backstepping, genetic algorithm, friction.

1. INTRODUCTION

In the field of mobile robotics, it is an accepted practice to work with kinematical models to obtain stable motion control laws for trajectory following or goal reaching (Fierro and Lewis, 1997; Khatib, *et al*., 1997). Some authors have proposed dynamic models relating the setpoints to the servos and the robot linear and angular velocities (Fukao, *et al*., 2000; Hu and Yang, 2001; Oriolo, *et al*., 2002; Rajagopalan and Barakat, 1997). Topalov, *et al*. (1998) use a model in which the torques of the servos appear as the input vector. Similarly, Yun and Yamamoto (1997) link the robot coordinates and the turned angle of each wheel with the servo's torques. In our paper a new dynamic model for differential drive mobile robots is presented.

The central problem in this paper is position tracking. In this case of dynamic mobile robot model, the position control law ought to be nonlinear in order to ensure the stability of the error, that is its convergence to zero (Hu and Yang, 2001; Oriolo, *et al*., 2002). Usually the backstepping method (Hu and Yang, 2001; Tanner and Kyriakopoulos, 2003) was used for obtaining a constructive quality nonlinear control. In order to achieve the optimal values of parameters that take place we used a genetic algorithm. Genetic algorithms provide non-linear robust search for spaces having many local minima and maxima. Holland (1992) established genetic algorithms as a viable technique that can be applied to a broad spectrum of problems. Genetic algorithms have been applied to various robotic control applications (Chin and Qi, 1996). This paper discusses the application of genetic algorithms to the tuning of nonlinear position tracking controller parameters.

The paper is organized as follows. In Section 2 the control system of mobile robot and its dynamic model are described. Section 3 contains the position and velocity control designs using a PI controller and nonlinear position control structure, respectively. Simulation results are presented and discussed in section 4. Some conclusions are given at the end of the paper.

2. CONTROL SYSTEM OF MOBILE ROBOT

The proposed control system with two-level controls is shown in Fig. 1. The low level velocity control system is composed of a multivariable PI controller and dynamic model of mobile robots and actuators. The medium level position control system generates a non-linear control law whose parameters are obtained using a genetic algorithm.

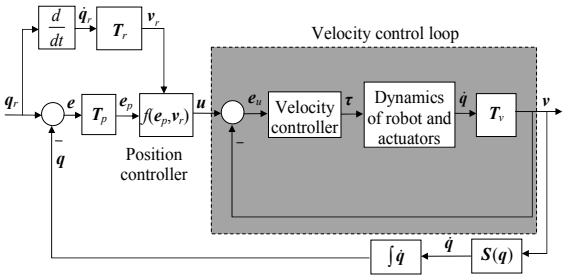

Fig. 1. Mobile robot position and velocity control .

Next, the basic motion analysis of the mobile robot will be performed.

2.1. Dynamics of Mobile Robot

In this section, a dynamic model of a nonholonomic mobile robot will be derived. A typical representation of a nonholonomic mobile robot is shown in Fig. 2.

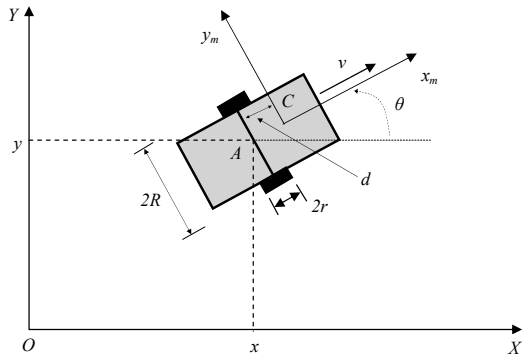

Fig. 2. The representation of a nonholonomic mobile robot.

The robot has two driving wheels mounted on the same axis and a free front wheel. The two driving wheels are independently driven by two actuators to achieve the motion and orientation. The position of the mobile robot in the global frame $\{X,O,Y\}$ can be defined by the position of the mass center of the mobile robot system, denoted by C, or alternatively by position A, which is the center of mobile robot gear, and the orientation between robot local frame $\{x_m,C,y_m\}$ and global frame. The kinetic energy of the whole structure is given by the following equation:

$$T = T_l + T_r + T_{kr}\,, \tag{1}$$

where T_l is a kinetic energy that is consequence of pure translation of the entire vehicle, T_r is a kinetic energy of rotation of the vehicle in XOY plane, and T_{kr} is the kinetic energy of rotation of wheels and rotors of DC motors. The values of introduced energy terms can be expressed by

$$T_l = \frac{1}{2}Mv_c^2 = \frac{1}{2}M(\dot{x}_c^2 + \dot{y}_c^2)\,, \tag{2}$$

$$T_r = \frac{1}{2}I_A\dot{\theta}^2\,, \tag{3}$$

$$T_{kr} = \frac{1}{2}I_0\dot{\theta}_R^2 + \frac{1}{2}I_0\dot{\theta}_L^2\,. \tag{4}$$

where M is the mass of the entire vehicle, v_c is linear velocity of the vehicle's center of mass C, I_A is the moment of inertia of the entire vehicle considering point A, θ is the angle that represents the orientation af the vehicle (Fig. 2), I_0 is the moment of inertia of the rotor/wheel complex and $d\theta_R/dt$ and $d\theta_L/dt$ are angular velocities of the right and left wheel respectively.

Further, the components of the velocity of the point A, can be expressed in terms of $d\theta_R/dt$ and $d\theta_L/dt$

$$\dot{x}_A = \frac{r}{2}(\dot{\theta}_R + \dot{\theta}_L)\cos\theta\,, \tag{5}$$

$$\dot{y}_A = \frac{r}{2}(\dot{\theta}_R + \dot{\theta}_L)\sin\theta\,, \tag{6}$$

$$\dot{\theta} = \frac{r(\dot{\theta}_R - \dot{\theta}_L)}{2R}\,. \tag{7}$$

Since $\dot{x}_C = \dot{x}_A - d\dot{\theta}\sin\theta$ and $\dot{y}_C = \dot{y}_A + d\dot{\theta}\cos\theta$, where d is distance between points A and C, it is obvious that following equations follow:

$$\dot{x}_C = \frac{r}{2}(\dot{\theta}_R + \dot{\theta}_L)\cos\theta - d\dot{\theta}\sin\theta\,, \tag{8}$$

$$\dot{y}_C = \frac{r}{2}(\dot{\theta}_R + \dot{\theta}_L)\sin\theta + d\dot{\theta}\cos\theta\,. \tag{9}$$

By substituting terms in Eq.1 with expressions in equations (2-9), total kinetic energy of the vehicle can be calculated in terms of $d\theta_R/dt$ and $d\theta_L/dt$:

$$T = T(\dot{\theta}_R,\dot{\theta}_R) = \frac{1}{2}A(\dot{\theta}_R^2 + \dot{\theta}_L^2) + B\dot{\theta}_R\dot{\theta}_L\,, \tag{10}$$

where

$$\begin{aligned} A &= \left(\frac{Mr^2}{4} + \frac{(I_A + Md^2)r^2}{4R^2} + I_0\right) \\ B &= \left(\frac{Mr^2}{4} - \frac{(I_A + Md^2)r^2}{4R^2}\right) \end{aligned}\,. \tag{11}$$

Now, the Lagrange equations ($L \equiv T$) can be written:

$$\frac{d}{dt}\left(\frac{\partial L}{\partial\dot{\theta}_R}\right) - \frac{\partial L}{\partial\theta_R} = \tau_R - K\dot{\theta}_R\,, \tag{12}$$

$$\frac{d}{dt}\left(\frac{\partial L}{\partial\dot{\theta}_L}\right) - \frac{\partial L}{\partial\theta_L} = \tau_L - K\dot{\theta}_L\,, \tag{13}$$

where τ_R and τ_L are the actuation torques (right and left) and $Kd\theta_R/dt$ and $Kd\theta_L/dt$ are the viscous friction torques of right and left wheel-motor systems, respectively.

Finally, the dynamic equations of motion can be expressed as:

$$A\ddot{\theta}_R + B\ddot{\theta}_L = \tau_R - K\dot{\theta}_R\,, \tag{14}$$

$$B\ddot{\theta}_R + A\ddot{\theta}_L = \tau_L - K\dot{\theta}_L\,, \tag{15}$$

3. POSITION AND VELOCITY CONTROL DESIGNS

The function of controller is to implement a mapping between the known information (e.g. reference position, velocity and sensor information) and the actuator commands designed to achieve the robot task. For a mobile robot, the controller design problem can be described as follows: given the reference position $\boldsymbol{q}_r(t)$ and velocity $\dot{\boldsymbol{q}}_r(t)$, design a control law for the actuator torques, which drive the mobile robot, so that the mobile robot velocity tracks a smooth velocity control input and the reference position. Let the velocity and position of the reference robot (Fig. 3) be given as:

$$\begin{aligned} \boldsymbol{q}_r &= [x_r y_r \theta_r]^T \\ \dot{x}_r &= v_r \cos\theta_r \\ \dot{y}_r &= v_r \sin\theta_r \\ \dot{\theta}_r &= \omega_r \end{aligned}, \qquad (16)$$

where v_r is the reference linear velocity and ω_r is the reference angular velocity.

3.1 Position Control

The trajectory tracking problem for a mobile robot is formulated with the introduction of a virtual reference robot (Egerstedt, *et al.*, 2001) to be tracked (Fig. 3). The tracking position error between the reference robot and the actual robot can be expressed in the robot frame as:

$$\boldsymbol{e}_p = \begin{bmatrix} e_1 \\ e_2 \\ e_3 \end{bmatrix} = \boldsymbol{T}_p \boldsymbol{e}_q = \begin{bmatrix} \cos\theta & \sin\theta & 0 \\ -\sin\theta & \cos\theta & 0 \\ 0 & 0 & 1 \end{bmatrix} \begin{bmatrix} x_r - x \\ y_r - y \\ \theta_r - \theta \end{bmatrix}, \qquad (17)$$

where $\boldsymbol{e}_q = [e_x \; e_y \; e_\theta]^T$.

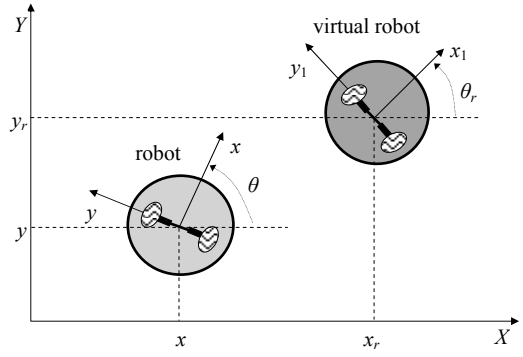

Fig. 3. The concept of tracking of a virtual reference robot.

The position error dynamics can be obtained from the time derivative of the (17) as:

$$\begin{aligned} \dot{e}_1 &= \omega e_2 + u_1, \\ \dot{e}_2 &= -\omega e_1 + v_r \sin e_3, \\ \dot{e}_3 &= u_2, \end{aligned} \qquad (18)$$

where inputs u_1 and u_2 are introduced.
In this paper we propose the following nonlinear control inputs as the servos for velocity control loop:

$$\begin{aligned} u_1 &= v_r \cos e_3 + \frac{k_1 e_1}{\sqrt{k_4 + e_1^2 + e_2^2}} \\ u_2 &= \omega_r + \frac{k_2 v_r e_2}{\sqrt{k_5 + e_1^2 + e_2^2}} + \frac{k_3 v_r \sin e_3}{\sqrt{k_6 + e_3^2}} \end{aligned}, \qquad (19)$$

where k_1, k_2, k_3, k_4, k_5 and k_6 are positive parameters. Equations (19) represent modified backstepping control law from (Hu and Yang, 2001), where denominators do not appear (they take value "1"). In (Hu and Yang, 2001), Lyapunov's stability theory was used to prove that the considered control law provides uniformly bounded norm of error $\|\boldsymbol{e}_p(t)\|$. The issue of rigorous proof of stability for introduced control law (19) remains open.
The key problem in such control design is to obtain control coefficients k_1 to k_6. To solve this problem, a genetic algorithm is used to find the optimal values of those coefficients. To apply this method a low-level velocity controller has to be designed first.

3.2 Velocity Control

The dynamics of the velocity controller is given by the following equations in Laplace domain:

$$\boldsymbol{\tau}(s) = \begin{bmatrix} \tau_R(s) \\ \tau_L(s) \end{bmatrix} = \frac{r}{2R} \begin{bmatrix} G_{11}(s) & G_{12}(s) \\ G_{21}(s) & G_{22}(s) \end{bmatrix} \begin{bmatrix} e_v(s) \\ e_\omega(s) \end{bmatrix}, \qquad (20)$$

where $e_v(s)$ is the linear velocity error, and $e_\omega(s)$ is the angular velocity error. This structure differs from previously used diagonal structures. Transfer functions $G_{ij}(s)$ are chosen to represent PI controllers:

$$\begin{aligned} G_{11}(s) &= K_1\left(1 + \frac{1}{T_{i1}s}\right) \cdot R, \; G_{12}(s) = K_2\left(1 + \frac{1}{T_{i2}s}\right) \\ G_{21}(s) &= K_1\left(1 + \frac{1}{T_{i1}s}\right) \cdot R, G_{12}(s) = -K_2\left(1 + \frac{1}{T_{i2}s}\right) \end{aligned}. \qquad (21)$$

The velocity control loop structure is shown in Fig. 1, as an inner loop. From the simulation results obtained (Figs. 4 and 5), it can be seen that the proposed PI controller successfully tracks the given linear and angular velocity profiles. These results justify the use of four controllers instead of two. The values for PI controller parameters are: K_1=100, K_2=60, T_{i1}=T_{i2}=20.

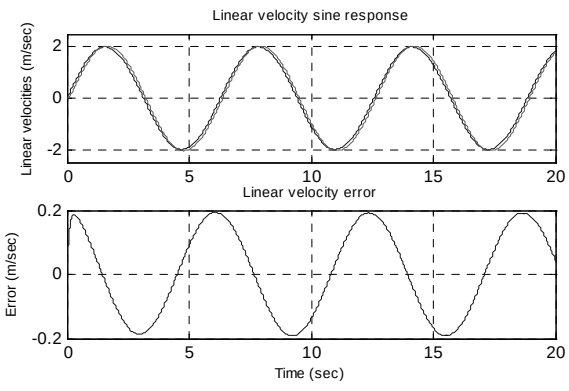

Fig. 4. Sine response of linear velocity and linear velocity error.

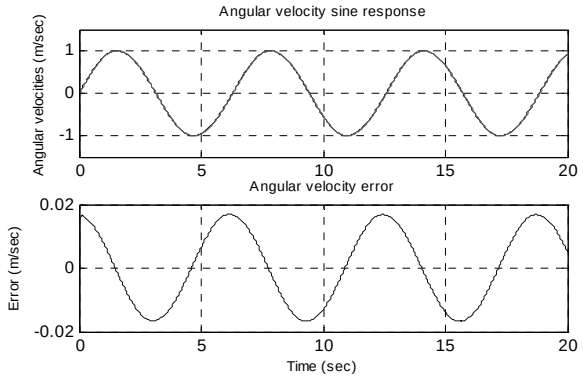

Fig. 5. Sine response of angular velocity and angular velocity error.

3.3 Evolution of the Coefficients

In this paper a simple genetic algorithm is used for parameter evolution. Coefficients k_1 to k_6 are encoded into a binary chromosome (Fig. 6).

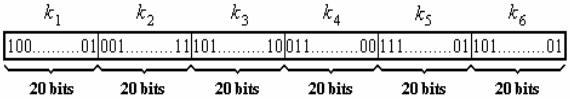

Fig. 6. Chromosome structure.

If $e_x(t)$, $e_y(t)$, and $e_\theta(t)$ ($0 < t < t_s$) are error functions, the objective function is calculated as in (22). Parameters a_x, a_y and a_θ are some positive real numbers. N is the number of error samples. The mapping between the objective and the fitness function has not been done, so it is obvious that the better individual has the smaller value of the objective function (fitness). In order to evaluate the fitness of the individual it is necessary to run the simulation.

$$F = a_x \sum_{i=0}^{N-1} \ln\left(1+\left|e_x\left(i\frac{t_s}{N}\right)\right|\right) + a_y \sum_{i=0}^{N-1} \ln\left(1+\left|e_y\left(i\frac{t_s}{N}\right)\right|\right) + a_\theta \sum_{i=0}^{N-1} \ln\left(1+\left|e_\theta\left(i\frac{t_s}{N}\right)\right|\right) \quad (22)$$

Values of the objective function parameters are: a_x= a_θ=1, a_y=2, N=1000 and t_s=10 sec.
In (22) we chosen the following criterion:

$$J_1 = \sum_{i=1}^{N} \ln\left(1+\left|e_i\right|\right), \quad (23)$$

rather than usually used ones, given by (24) and (25)

$$J_2 = \sum_{i=1}^{N} \left|e_i\right|, \quad (24)$$

$$J_3 = \sum_{i=1}^{N} e_i^2 \ . \quad (25)$$

The criterion J_1 penalizes smaller errors (expected in the stationary state) more (Fig. 7) and consequently it ensures the better position tracking.
Error $e_\theta(t)$ is calculated as follows:

$$e_\theta = \begin{cases} \theta_r - \theta, \text{ if } \left|\theta_r-\theta\right| < \min\left(\left|\theta_r-\theta-2\pi\right|, \left|\theta_r-\theta+2\pi\right|\right) \\ \theta_r - \theta - 2\pi, \text{ if } \left|\theta_r-\theta-2\pi\right| < \min\left(\left|\theta_r-\theta\right|, \left|\theta_r-\theta+2\pi\right|\right) \\ \theta_r - \theta + 2\pi, \text{ if } \left|\theta_r-\theta+2\pi\right| < \min\left(\left|\theta_r-\theta\right|, \left|\theta_r-\theta-2\pi\right|\right) \end{cases} \quad (26)$$

This type of error is suitable since it prevents unnecessary full circle rotation.

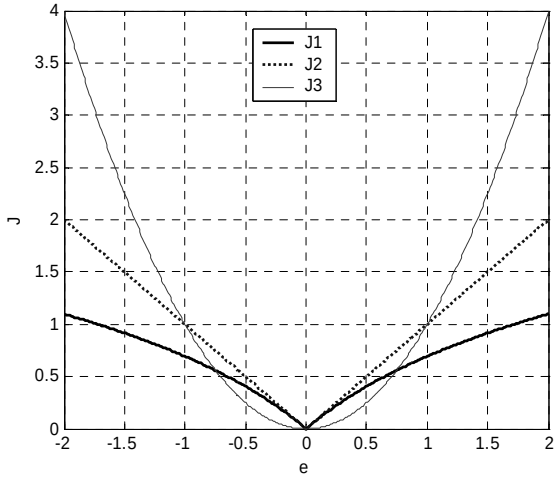

Fig. 7. Graphical illustration of different criteria.

The coefficient evolution is performed using a lemniscate as suitable complex trajectory:

$$x_r(t) = \frac{a\sin(\alpha t)}{1+\sin^2(\alpha t)}$$
$$y_r(t) = \frac{a\sin(\alpha t)\cos(\alpha t)}{1+\sin^2(\alpha t)}, \quad (27)$$
$$\theta_r(t) = \arctan\left(\frac{\dot{y}_r(\alpha t)}{\dot{x}_r(\alpha t)}\right)$$

where a=α=1.The evolution process (population size is 40) is depicted in Fig. 8.

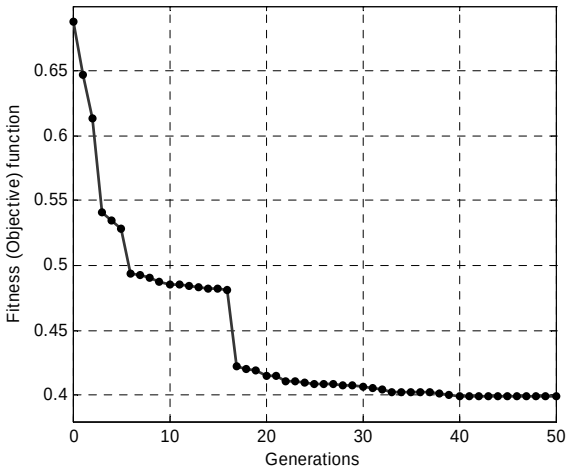

Fig. 8. Change of the best fitness in the population through generations.

This evolution yielded the following values for considered coefficients: K_1=6.2457, K_2=221.2306, K_3=2.3433, K_4=13.5117, K_5=3.1933, K_6=8.3361.

4. SIMULATION RESULTS

In this section, the above controller is applied to the dynamic model of the robot derived in this paper. The Simulink model of the mobile robot control system is shown in Fig. 7. The used mobile robot parameters are M=10kg, I_A=1kgm^2, r=0.035 m, R=0.175 m, d=0.05 m, m_0=0.2 kg , J_0=0.0001 kgm^2, K/A=0.1, and are the same that have been during the evolution.

Two trajectories are selected to verify the performance of the proposed control system: a circular and a lemniscate path. The results of the trajectory tracking task in both cases are shown in Figs. 9-11 and Figs. 12-14, respectively. From these figures, it can be concluded that satisfactory tracking results are obtained using the proposed control system.

Finally, the comparison of Cartesian error norm profiles has been presented for different friction coefficients in Fig. 15. This experiment has been done for a lemniscate path. It is obvious that the friction increase causes degradation of control system performance.

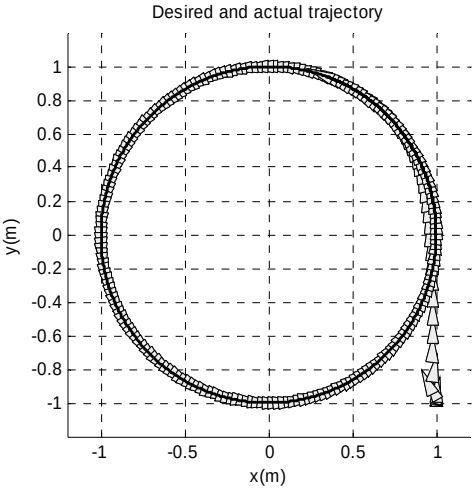

Fig. 9. Tracking a circular path.

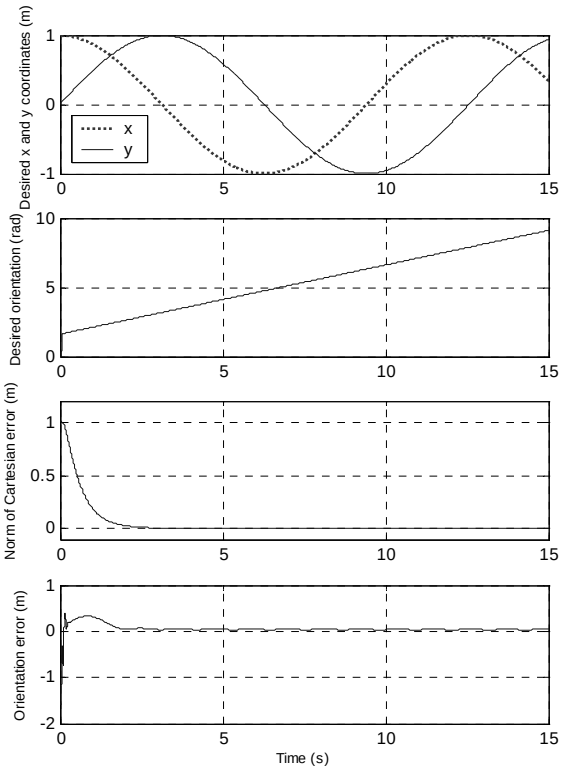

Fig. 10. Time diagrams for important variables (circular trajectory)

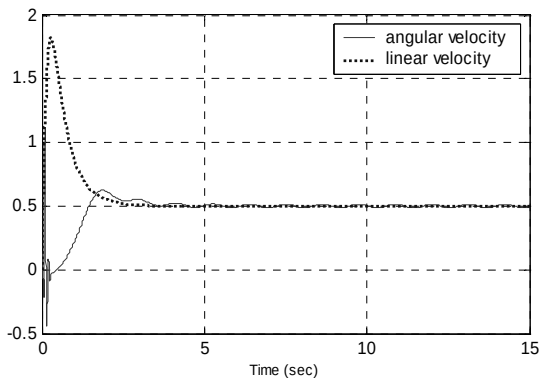

Fig. 11. Velocity profiles (circular trajectory).

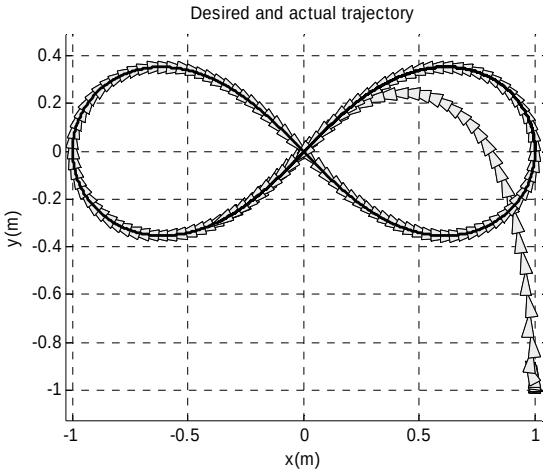

Fig. 12. Tracking a lemniscate path.

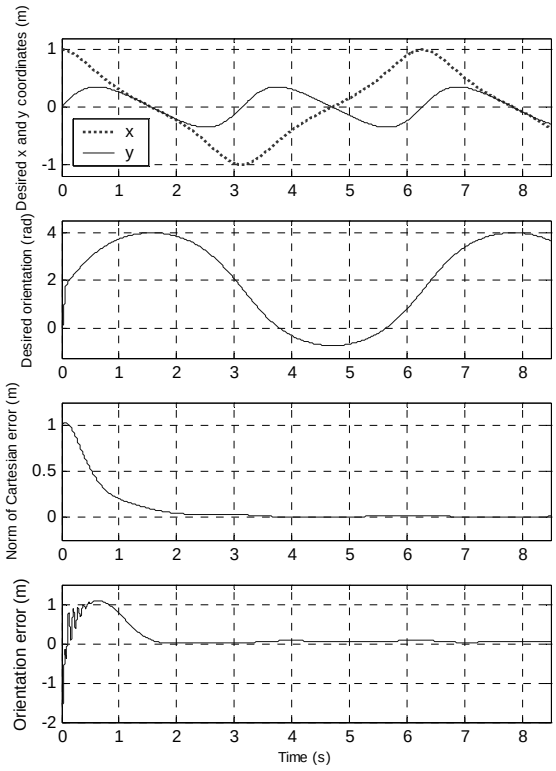

Fig. 13. Time diagrams for important variables (lemniscate trajectory)

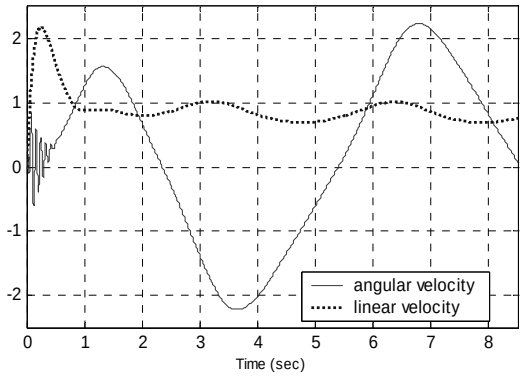

Fig. 14. Velocity profiles (lemniscate trajectory)

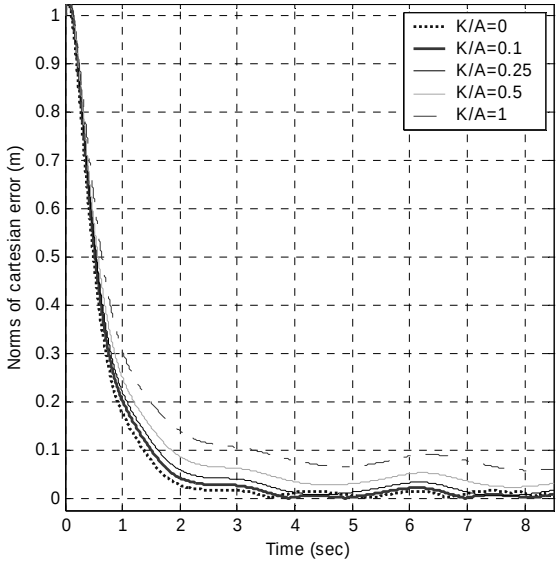

Fig. 15. Norms of Cartesian error for various friction coefficients

5. CONCLUSIONS

In this paper a new dynamic model of a mobile robot with nonholonomic constraints is derived first. The special feature of this model is that main variables are angular velocities of wheels. Due to this approach the impossibility of the lateral motion is embedded into the model. In addition such a model is easily simulated.

The overall control system has an inner velocity loop based on PI controllers. The coefficients of the outer nonlinear modified backstepping position control loop are adjusted by a genetic algorithm. The efficiency of obtained controller is demonstrated on various trajectory tracking.

The future work will explore some other methods of nonlinear position control laws. One alternative approach may be replacing the backstepping control law with a feedforward neural network, learned with a genetic algorithm.

REFERENCES

Fierro, R. and F.L. Lewis (1997). Control of a Nonholonomic Mobile Robot: Backstepping Kinematics into Dynamics. *Journal of Robotics Systems*, **Vol. 14**, pp. 149–163.

Khatib, M., H. Jaouni, R. Chatila, and J.P. Laumond (1997). Dynamic Path Modification for Car-Like Nonholonomic Mobile Robots. In: *Proceedings of the IEEE International Conference on Robotics and Automation*, pp. 2920–2925.

Fukao, T, H. Nakagawa, and N. Adachi (2000). Adaptive Tracking Control of a Nonholonomic Mobile Robot, *IEEE Transaction on Robotics and Automation*, **Vol. 16**, pp. 609-615.

Hu, T. and S.X. Yang (2001). Real-time Motion Control of a Nonholonomic Mobile Robot with Unknown Dynamics. In: *Proceedings of the Computational Kinematics Conference*, Seoul.

Oriolo, G., A. De Luca and M. Vendittelli (2002). WMR control via dynamic feedback linearization: Design, implementation and experimental validation. *IEEE Transactions on Control System Technology*, **Vol. 10**, pp. 835-852.

Rajagopalan, R. and N. Barakat (1997). Velocity Control of Wheeled Mobile Robots Using Computed Torque Control and Its Performance for a Differentially Driven Robot. *Journal of Robotic Systems*, **Vol. 14**, pp. 325-340.

Topalov, A.V., D.D. Tsankova, M.G. Petrov, and T. Proychev (1998). Intelligent Sensor-Based Navigation and Control of Mobile Robot in a Partially Known Environment. In: *Proceedings of the 3rd IFAC Symposium on Intelligent Autonomous Vehicles*, pp. 439–444.

Yun, X. and Y. Yamamoto (1997). Stability Analysis of the Internal Dynamics of a Wheeled Mobile Robot. *Journal of Robotics Systems*, **Vol. 14**, pp. 698–709.

Tanner, H.G. and K.J. Kyriakopoulos (2003). Backstepping for nonsmooth systems. *Automatica*, **Vol. 39**, pp. 1259-1265.

Holland, J.H. (1992). *Adaptation in Natural Artificial Systems*, University of Michigan Press, Michigen.

Chin, T.C. and X.M. Qi, (1996). Integrated Genetic Algorithms based Optimal Fuzzy Logic Controller Design. In: *Proceedings of the Fourth International Conference on Control, Automation, Robotics and Vision*, pp. 563-567.

Egerstedt, M., X. Hu, and A. Stotsky (2001). Control of Mobile Platforms Using a Virtual Vehicle Approach. *IEEE Transaction on Automatic Control*, **Vol. 46**, pp. 1777-1882.